*Chem Biol Drug Des 2010;* **76:** 43–58

Research Article



doi: 10.1111/j.1747-0285.2010.00978.x

# Insights into the *In Vitro* Antitumor Mechanism of Action of a New Pyranoxanthone

**Andreia Palmeira[1,2,3], Ana Paiva[1,2], Emília Sousa[1,2], Hugo Seca[3], Gabriela M. Almeida[3], Raquel T. Lima[3,4], Miguel X. Fernandes[5], Madalena Pinto[1,2] and M. Helena Vasconcelos[2,3,4,*]**

*[1]Department of Chemistry, Laboratory of Organic and Pharmaceutical Chemistry, Faculty of Pharmacy, University of Porto, Rua Anibal Cunha 164, 4050-047 Porto, Portugal*
*[2]Research Center of Medicinal Chemistry (CEQUIMED-UP), University of Porto, Rua Anibal Cunha 164, 4050-047 Porto, Portugal*
*[3]Cancer Biology Group, IPATIMUP – Institute of Molecular Pathology and Immunology of the University of Porto, Rua Dr. Roberto Frias, S/N, 4200-465 Porto, Portugal*
*[4]Department of Biological Sciences, Laboratory of Microbiology, Faculty of Pharmacy, University of Porto, Rua Anibal Cunha 164, 4050-047 Porto, Portugal*
*[5]Centro De Química da Madeira, Universidade da Madeira, Campus da Penteada, 9000-390 Funchal, Portugal*
**Corresponding author: M. Helena Vasconcelos, hvasconcelos@ipatimup.pt*

**Naturally occurring xanthones have been documented as having antitumor properties, with some of them presently undergoing clinical trials. In an attempt to improve the biological activities of dihydroxyxanthones, prenylation and other molecular modifications were performed. All the compounds reduced viable cell number in a leukemia cell line K-562, with the fused xanthone 3, 4-dihydro-12-hydroxy-2,2-dimethyl-2*H*,6*H*-pyrano[3, 2-b]xanthen-6-one (5) being the most potent. The pyranoxanthone 5 was particularly effective in additional leukemia cell lines (HL-60 and BV-173). Furthermore, the pyranoxanthone 5 decreased cellular proliferation and induced an S-phase cell cycle arrest. *In vitro*, the pyranoxanthone 5 increased the percentage of apoptotic cells which was confirmed by an appropriate response at the protein level (e.g., PARP cleavage). Using a computer screening strategy based on the structure of several anti- and pro-apoptotic proteins, it was verified that the pyranoxanthone 5 may block the binding of anti-apoptotic Bcl-xL to pro-apoptotic Bad and Bim. The structure-based screening revealed the pyranoxanthone 5 as a new scaffold that may guide the design of small molecules with better affinity profile for Bcl-xL.**

**Key words:** antiproliferation, apoptosis, Bcl-xL, leukemia, structure-based screening, xanthone

Received 21 October 2009, revised 11 March 2010 and accepted for publication 16 March 2010

A large number of naturally occurring and synthetic xanthones with interesting biological and pharmacological activities have been reported in the past few years, namely as antitumor agents (1). The most remarkable examples undergoing clinical trials as antitumor agents are psorospermin (**1**), a fused furanoxanthone, a promising antileukemic agent isolated from the roots and bark of the tropical African plant *Psorospermum febrifugum* (2), and dimethylxanthenone-4-acetic acid (DMXAA, **2**) which causes a fast vascular collapse and tumor necrosis and was discovered in a structure–activity relationship study involving a series of flavone acetic acid analogues (3,4) (Figure 1). Natural dehydroxanthones namely artobiloxanthone (5) and caged xanthones like gaudichaudione A (6) are also potent antileukemia agents. The significant antitumor properties reported for the dehydrofuranoxanthone psorospermin (**1**) as well as for the acridone alkaloid acronycine (**3**, Figure 1), both linear tricyclic ring systems fused to a fourth oxygenated ring, had already encouraged the investigation into isosteric acronycine xanthone derivatives that were even more potent than acronycine (**3**) in L1210 leukemia cell line (7–9). Nevertheless, acronycine (thio)xanthone derivatives with methoxy group in the 1-position were found to be highly insoluble and did not improve the overall activity (8,10).

Xanthones with prenyl units, either fused in a ring or as an open-chain unit, have been reported to mediate some important biological activities, concerning a large variety of targets with therapeutic value (1,11). In our research group, we have previously investigated the effect of several prenylated derivatives of 1,3-dihydroxy-2-methylxanthone and 1,3-dihydroxyxanthone on the *in vitro* growth of some human tumor cell lines, with particular attention on breast adenocarcinoma (MCF-7) (12). It was found that, in some cases, the presence of prenyl side chains enhanced activity when compared with their non-prenylated analogs (12,13).

Considering previous results and the fact that 3,4-dihydroxyxanthone (**4**), interesting as a PKC inhibitor (14) but with limited growth inhibitory effects on human tumor cell lines (15) is more water-soluble than the previously investigated oxygenated scaffolds (8,10,12), the synthesis of both open-chain and fused prenylated derivatives of compound **4** was initially planned to look for antileukemic agents (Figure 2). Herein, we firstly describe the synthesis and effect on the viable cell number of a leukemia cell line, of a dihydropyrano

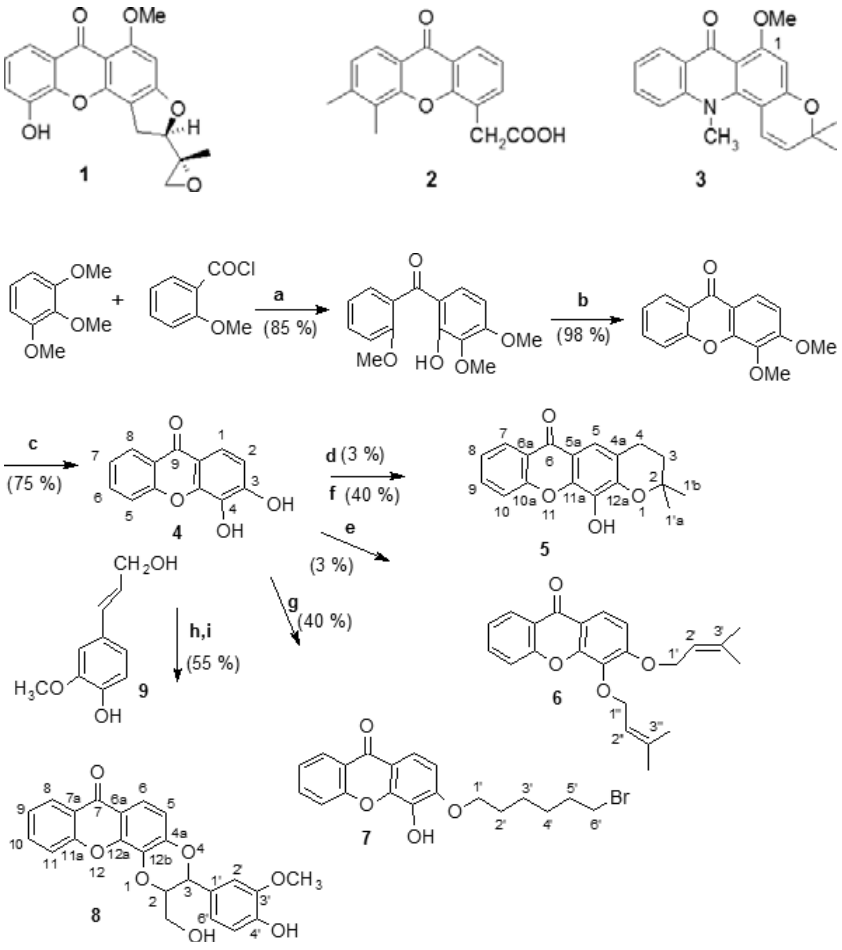


**Figure 1:** Structures of antitumor xanthones in clinical trials (**1**–**2**) and of acronycine (**3**).

**Figure 2:** Synthesis of 3,4-dihydroxyxanthone (**4**) analogues **5**–**8**. (**a**) $Et_2O$, $AlCl_3$, room temp, 22 h; (**b**) MeOH, $H_2O$, NaOH, reflux, 47 h; (**c**) $C_6H_5CH_3$, $AlCl_3$, 70 °C, 13 h; (**d**) $BrCH_2CHC(CH_3)_2$, MW 200 W, Montmorillonite K10 (20 equiv.), $CHCl_3$, 40 min; (**e**) $BrCH_2CHC(CH_3)_2$, $K_2CO_3$, DMF, room temp, 48 h; (**f**) $Br(CH_2)_6Br$ (drop-wise, 30 min), $K_2CO_3$, DMF, room temp, 24 h; (**g**) $K_3[Fe(CN)_6]$, $Me_2CO$:$H_2O$ (1:1), room temp; (**h**) $K_2CO_3$, $H_2O$, room temp.

(**5**) and a diprenylated derivative (**6**), as well as of the bromoalkylated (**7**) and the fused lignoid (**8**) derivatives of 3,4-dihydroxyxanthone (**4**). The effect of the most potent compound, the fused xanthone 3,4-dihydro-12-hydroxy-2,2-dimethyl-2*H*,6*H*-pyrano[3,2-b]xanthen-6-one (**5**), on viable cell number was also confirmed in additional leukemia cell lines.

To gain further insights into the mechanism of action of the fused xanthone derivatives, the antiproliferative and apoptotic effects of compound **5** were evaluated, and docking studies were further performed.

## Materials and Methods

### *Chemistry*

$K_3[Fe(CN)_6]$ was supplied by Merck (Darmstadt, Germany). Prenyl bromide, dibromohexane, and coniferyl alcohol (**9**) were obtained from Sigma (Steunheim, Germany). Purifications of compounds **4**–**8** were performed by column chromatography (CC) using Merck silica gel 60 (0.040–0.063 mm) and preparative thin layer chromatography (TLC) using Merck silica gel 60 (GF254) plates. Microwave reactions were performed using set-up for atmospheric-pressure reactions and also 120 mL closed reactors (internal reaction temperature measurement with a fiber-optic probe sensor) and were carried out using an Ethos MicroSYNTH 1600 Microwave Labstation (Milestone). Melting points were obtained in a Köfler microscope (Wagner and Munz, Munich, Germany) and are uncorrected. The optical rotation was zero for **8** and was obtained on a Polartronic Universal polarimeter. IR spectra were measured on an ATI Mattson Genesis series FTIR (software: WinFirst v.2.10) spectrophotometer in KBr microplates. $^1H$ and $^{13}C$ NMR spectra were taken in $CDCl_3$ or DMSO-$\delta$6 at room temperature, on Bruker Avance 300 instrument (300.13 MHz for $^1H$ and 75.47 MHz for $^{13}C$). Chemical shifts are expressed in $\delta$ (ppm) values relative to tetramethylsilane (TMS) as an internal reference; $^{13}C$ NMR assignments were made by 2D heteronuclear single quantum correlation (HSQC) and Hetronuclear Multiple Bond Correlation (HMBC) experiments (long-range C, H coupling constants were optimized to 7 and 1 Hz). Mass spectrometry (MS) spectra were recorded as electronic impact (EI) mode on a VG Autospec Q spectrometer, and high resolution mass spectrometry (HRMS) results were obtained in the services of C.A.C.T.I. (Vigo, Spain). The following materials were synthesized and purified by the described procedures.

**3,4-Dihydroxyxanthone (4)** The synthesis of compound **4** (Figure 2) was carried out according to the method of Gottlieb *et al.* (16). To the crude product obtained from the demethylation of 3,4-dimethoxyxanthone, HCl 5N (80 ml) was added, and the mixture was extracted with ethyl acetate. The organic layer was collected

and dried ($Na_2SO_4$), and the solvent was evaporated to dryness. Compound **4** was isolated by crystallization from acetone/petroleum ether (40–60 °C boiling fraction) (4:1 v/v) as slightly yellow crystals (70%) and characterized according to the described procedure (14).

### 3,4-Dihydro-12-hydroxy-2,2-dimethyl-2*H*,6*H*-pyrano[3,2-b]xanthen-6-one (5)

A mixture of **4** (4.4 mmol), prenyl bromide (8.8 mmol), and anhydrous $K_2CO_3$ (9.0 mmol) in anhydrous dimethylformamide (DMF) (20 mL) was refluxed for 8 h (150 °C). After cooling, the solid was filtered and the solvent removed under reduced pressure and afforded the crude product that was purified by flash chromatography ($SiO_2$; hexane/AcOEt, 6:4 v/v) and by preparative TLC ($SiO_2$; hexane/AcOEt, 5:5 v/v). Yellow crystals of **5** were obtained from acetone (3%). This procedure was optimized to get procedure **f**: A slurry of the K10 clay (20 equiv of weight) in $CHCl_3$ (ca. 30 mL) was treated with the 3,4-dihydroxyxanthone (**4**, 3.55 mmol), followed by the addition of prenyl bromide (14.20 mmol) in $CHCl_3$, in a 120-mL microwave reactor. The mixture under stirring was irradiated at 200 W for 2 × 20 min, and the final temperature was 108 °C. The reaction mixture was filtered under vacuum, washed with $CH_2Cl_2$, $Me_2CO$, and MeOH, and the filtrate was concentrated under vacuum. The recovered clay was reactivated by washing with MeOH. The crude product was purified by chromatography flash cartridge (Grace Resolv®, Grace Company, Deerfield, IL, USA) in hexane/AcOEt (7:3 v/v). Yellow crystals of compound **5** were obtained from acetone (518 mg, 40%): mp 199–202 °C ($Me_2CO$); $^1$H-NMR ($CDCl_3$): $\delta$ = 8.33 (1H, dd, *J* = 8.0 and 1.6 Hz, H-7), 7.70 (1H, ddd, *J* = 7.7, 8.0, and 1.6 Hz, H-9), 7.70 (1H, s, H-5), 7.58 (1H, dd, *J* = 8.0 and 1.0 Hz, H-8), 7.35 (1H, ddd, *J* = 7.3, 7.3, and 1.0 Hz, H-10), 5.74 (1H, br s, OH); 2.93 (2H, t, *J* = 6.7, H-4), 1.92 (2H, t, *J* = 6.7, H-3), 1.45 (6H, s, H-1′) ppm; $^{13}$C-NMR ($CDCl_3$): $\delta$ = 176.7 (C-6), 156.1 (C-10a), 146.3 (C-12a), 143.2 (C-11a), 134.3 (C-9), 132.4 (C-12), 126.6 (C-7), 123.6 (C-8), 121.5 (C-6a), 118.2 (C-10), 117.9 (C-5), 117.0 (C-4a), 115.4 (C-5a), 76.5 (C-2), 32.6 (C-3), 27.0 (C-4), 21.7 (C-1′) ppm; IR (KBr): $\nu$ = 3315, 2867, 2924, 2851, 1653, 1611, 1455, 1370, 1253, 1222, 1190, 1154, 1117, 757 cm$^{-1}$; MS (EI, 70 eV) *m/z* (%): 296 (98) $[M]^+$, 241 (100), 209 (28), 156 (15), 128 (15), 73 (5); HRMS-ESI *m/z* calcd for $C_{18}H_{16}O_4$ $[M-H]^+$ 296.1049, found: 296.1051.

### 3,4-*bis*-(3-Methylbut-2-enyloxy)-9*H*-xanten-9-one (6)

To a solution of **4** (2.2 mmol) in dry DMF (15 mL) and $K_2CO_3$ (4.4 mmol), prenyl bromide (4.4 mmol) was added drop-wise, with stirring at room temperature. After 8 h, the reaction mixture was poured into ice-water (50 mL), and the solid was filtered. From this crude product, the compound **6** was isolated by preparative TLC ($SiO_2$; hexane/AcOEt, 6:4 v/v). Prenylated xanthone **6** was crystallized as a brown powder from EtOH (20 mg, 3%): mp > 330 °C (EtOH); $^1$H-NMR ($CDCl_3$): $\delta$ = 8.32 (1H, dd, *J* = 8.0 and 1.8 Hz, H-8), 8.06 (1H, d, *J* = 9.0 Hz, H-1), 7.70 (1H, ddd, *J* = 7.0, 9.0, and 1.6 Hz, H-6), 7.56 (1H, dd, *J* = 8.3 and 1.0 Hz, H-7), 7.37 (1H, ddd, *J* = 6.0, 7.5, and 1.0, H-5), 7.00 (1H, d, *J* = 9.0 Hz, H-2), 5.65 (1H, t, *J* = 6.6 Hz, H-2′), 5.53 (1H, t, *J* = 7.4 Hz, H-2″), 4.73 (2H, d, *J* = 6.6 Hz, H-1′), 4.67 (2H, *J* = 7.4 Hz, H-1″), 1.80 (6H, s, H-3′), 1.74 (6H, s, H-3″) ppm; $^{13}$C-NMR ($CDCl_3$): $\delta$ = 177.4 (C-9), 157.5 (C-4b), 151.1 (C-3), 139.5 (C-4a), 138.6 (C-3′), 136.4 (C-4), 135.4 (C-3″), 134.4 (C-6), 126.6 (C-8), 123.8 (C-7), 122.1 (C-2″), 121.5 (C-8a), 120.0 (C-2′), 119.1 (C-2″), 118.8 (C-8a), 118.6 (C-9a), 118.2 (C-5),118.0 (C-1), 116.5 (C-2), 69.8 (C-1′), 66.1 (C-1″), 25.8 (3′-$CH_3$), 25.7 (3″-$CH_3$), 18.3 (3′-$CH_3$), 17.9 (3″-$CH_3$) ppm; IR (KBr): $\nu$ = 3408, 2959, 2920, 2852, 1655, 1603, 1463, 1436, 1375, 1330, 1282, 1261, 1222, 1077, 756 cm$^{-1}$; MS (EI, 70 eV) *m/z* (%): 364 (54), 349 (74), 239 (100), 225 (78), 211 (63), 197 (35), 121 (20), 65 (6); HRMS-ESI *m/z* calcd for $C_{23}H_{25}O_4$ $[M-H]^+$ 365.1756; found: 365.1747.

### 3-[(6′-Bromohexyl)oxy]-4-hydroxy-9*H*-xanthen-9-one (7) (17)

To a solution of compound **4** (2.2 mmol) in dry DMF (10 mL), was added $K_2CO_3$ (2.2 mmol), and the mixture was stirred at room temperature for 15 min. To this suspension was added, in 30 min, a solution of 1,6-dibromobutane (4.4 mmol) in dry DMF (5 mL). The reaction mixture was stirred for 8 h at room temperature and then poured into ice-water (50 mL). The brown solid thus obtained was filtered and purified by CC [petroleum ether (40–60 °C boiling fraction)/diethyl ether, several proportions]. A white solid was obtained from the collected fractions from petroleum ether/diethyl ether (4:6 v/v). Crystallization from ethyl acetate/petroleum ether (3:1 v/v) gave compound **7** (345 mg, 40%): mp 173 °C (ethyl acetate/petroleum ether); $^1$H-NMR (DMSO-$\delta$6): $\delta$ = 8.34 (1H, dd, J = 8.0 and 1.6 Hz, H-8), 7.91 (1H, d, *J* = 8.9 Hz, H-1), 7.73 (1H, ddd, *J* = 7.0, 7.0, and 1.5 Hz, H-6), 7.60 (1H, d, *J* = 7.9 Hz, H-5), 7.38 (1H, ddd, J = 7.0, 7.0, and 1.5 Hz, H-7), 6.99 (1H, d, J = 8.9 Hz, H-2), 5.75 (1H, s, HO-C(4)), 4.23 (2H, t, H-1′), 3.44 (2H, t, H-6′), 1.93 (4H, m,H-2′ and H-5′), 1.59 (4H, m, H-3′ and H-4′) ppm; $^{13}$C NMR (DMSO-$\delta$6): $\delta$ = 175.1 (C-9), 166.0 (C-10a), 150.3 (C-3), 144.9 (C-4a), 134.6 (C-6), 133.5 (C-4), 126.7 (C-8), 123.9 (C-7), 121.6 (C-8a), 118.2 (C-5), 118.2 (C-1), 116.6 (C-9a), 108.3 (C-2), 69.5 (C-1′), 33.7 (C-6′), 32.9 (C-2′), 29.7 (C-5′), 28.0 (C-3′), 25.1 ppm (C-4′); IR (KBr): $\nu$ = 1645, 1606, 1455, 1334, 1250, 1184, 1081, 757 cm$^{-1}$; HRMS-ESI *m/z* calcd for $C_{19}H_{20}BrO_4$ $[M-H]^+$ 391.05395, found: 391.05375.

### (±)-(2*R**,3*R**)- and (±)-(2*S**,3*S**)-2-Hydroxymethyl-3-(4-hydroxy-3-methoxyphenyl)-1,4-dioxane[5,6-c]xanthones (8)

To a stirred solution of **4** (11.5 mmol) and **9** (11.1 mmol) in a 1:1 mixture of $Me_2CO/H_2O$ (250 mL), a AcONa solution (44 mmol, in 100 mL of $H_2O$) and then a $K_3[Fe(CN)_6]$ solution (120 mmol in $H_2O$) were added, at room temp. After 5 h, the mixture was slightly acidified with 10% HCl and the precipitate filtrated. The product obtained, corresponding to a mixture of *trans* and *cis* isomers of **8** (3 g), was suspended in $H_2O$ (250 mL) and basified with $K_2CO_3$. The suspension was stirred at room temp, for 1 day, until complete conversion of *cis* isomer into the *trans* isomer of **8**. The product was filtered, washed with $H_2O$, dried, and crystallized from 1,4-dioxane to get a white powder (2.5 g, 55%): mp 243–245 °C (1,4-dioxane); $^1$H-NMR (DMSO-$\delta$6): $\delta$ = 9.25 (1H, s, C(4′)-O*H*), 8.20 (1H, dd, *J* = 7.7 and 1.6 Hz, H-8), 7.87 (1H, ddd, *J* = 8.3, 7.4, and 1.6 Hz, H-10), 7.70 (1H, d, *J* = 8.8 Hz, H-6), 7.69 (1H, d, *J* = 8.3 Hz, H-11), 7.49 (1H, ddd, *J* = 7.7, 7.4, and 0.7 Hz, H-9), 7.07 (1H, d, *J* = 8.8 Hz, H-5), 7.07 (1H, d, *J* = 1.7 Hz, H-2′), 6.92 (1H, dd, *J* = 8.1 and 1.7 Hz, H-6′), 6.83 (1H, d, *J* = 8.1 Hz, H-5′), 5.15 (1H, d,

$J$ = 7.9 Hz, H-2), 5.13 (1H, t, $J$ = 6.1 Hz, $CH_2OH$), 4.36-4.40 (1H, m, H-3), 3.79 (3H, s, 3′-$OCH_3$), 3.71-3.76 (1H, m, C$H_2$OH), 3.40-3.50 (1H, m, 2-$CH_2$) ppm; $^{13}$C-NMR (DMSO-$\delta$6): $\delta$= 175.1 (C-7), 155.4 (C-11a), 148.8 (C-4a), 147.7 (C-3′), 147.2 (C-4′), 145.9 (C-12a), 135.2 (C-10), 131.8 (C-12b), 126.7 (C-1′), 126.0 (C-8), 124.5 (C-9), 121.0 (C-7a), 120.7 (C-6′), 118.1 (C-11), 117.5 (C-6), 115.7 (C-6a), 115.4 (C-5′), 113.9 (C-5), 111.8 (C-2′), 78.0 (C-3), 76.5 (C-2), 59.9 (2-$CH_2$), 55.7 (3′-$OCH_3$) ppm; IR (KBr): $\nu$ = 3398, 1642, 1605, 1562, 1449, 1338, 1264, 1025, 861 cm$^{-1}$; MS (EI, 70 eV) $m/z$ (%): 406 (6) [M$^+$], 356 (26), 341 (22), 327 (17), 306 (18), 292 (12), 281 (100), 261 (38), 253 (5), 228 (13), 215 (8), 180 (10), 165 (8), 141 (10), 115 (18), 105 (9), 91 (17), 77 (18), 63 (10), 55 (13); HRMS-ESI $m/z$ calcd for $C_{23}H_{19}O_7$ [M-H]$^+$ 407.1131, found: 407.1130.

### Cell lines

K-562 (human chronic myelogenous leukemia, erythroblastic), HL-60 (human acute myelocytic leukemia), BV-173 (human chronic myeloid leukemia, lymphoid), and MRC-5 (immortalized fibroblasts) cell lines were routinely maintained in RPMI-1640 (with Hepes and Glutamax; Gibco® Invitrogen Cell Culture, Barcelona, Spain), with 10% fetal bovine serum (FBS; Gibco) and incubated in a humidified incubator at 37 °C with 5% $CO_2$ in air. All experiments were performed with cells in exponential growth with viabilities over 90% and repeated at least three times.

### Cellular response to the compounds in terms of viable cell number

In the experiments to determine the cellular response of K-562 cells to different compounds, cells were plated ($2 \times 10^5$ cells/mL in 24-well plates) and treated with complete medium (blank), with the solvent of the compounds (DMSO 0.2% v/v, control), or with the following compounds: **4**, **6**–**8** (10 and 20 $\mu$M) and **5** (1, 2.5, 5, 10 and 20 $\mu$M). For further verification of the effects of the pyranoxanthone **5**, the HL-60 and BV-173 cell lines were plated under the same conditions described for K-562 cells and were treated with compound **5** (5, 10 and 20 $\mu$M). For the experiments with the adherent cell line, MRC-5, compound **5** (10 or 20 $\mu$M) was added to the cells only 24 h after plating ($2 \times 10^5$ cells/mL in 6-well plates). For all cell lines, viability and cell number were assessed following 24, 48, and 72 h of incubation with the compounds, using the trypan blue exclusion assay. The equivalent volume of the compounds solvent (DMSO) was added to the cells and analyzed at the same time-points, as a control.

### Cellular proliferation analysis by the BrdU incorporation assay

To assess the effect of the pyranoxanthone **5** on K-562 cellular proliferation, BrdU incorporation was analyzed 72 h after incubation with complete medium (blank), with the solvent of the compounds (DMSO 0.2% v/v, control), or with compound **5** (10 or 20 $\mu$M). After a pulse of BrdU (10 $\mu$M, Sigma) for 1 h, cells were washed, fixed in 4% paraformaldehyde in phosphate buffer saline (PBS), and cytospins prepared. After incubation in 2M HCl for 20 min, cells were incubated with mouse anti-BrdU (1:10, Dako®, Glostrup, Denmark) and further incubated with fluorescein-labeled rabbit anti-mouse antibody (1:100, Dako). For nuclear counter staining, Vectashield mounting medium for fluorescence with 4′,6-diamidino-2-phenylindole (DAPI; Vector Laboratories Inc., Peterborough, UK) was used. Cells were observed in a LEICA DM2000 microscope (LEICA), and a semiquantitative evaluation was performed by counting a minimum of 300 cells per slide.

### Cell cycle analysis

For the analysis of cell cycle phase distribution of DNA, K-562 cells were treated as indicated earlier with complete medium (blank), the solvent of the compounds (DMSO 0.2% v/v, control), or with compound **5** (10 or 20 $\mu$M) and processed at 48 and 72 h after incubation with the compounds. Cells were pelleted and fixed in 70% ethanol for 10 min at room temperature. After centrifugation, cells were stained for 30 min on ice in propidium iodide (40 $\mu$g/mL) and RNase in PBS (100 $\mu$g/mL). At least 50 000 cells per sample were counted and analyzed by flow cytometry (Epics XL-MCL; Beckman Coulter, Brea, CA, USA), and the percentage of cells in the G1, S, and G2/M phases of the cell cycle was determined using the FlowJo 7.2 software (Tree Star Inc., Ashland, OR, USA) after cell debris exclusion.

### Cellular apoptosis analysis by the TUNEL assay

The levels of apoptosis of the K-562 cells treated with compound **5** were analyzed by the TUNEL assay, using the *In Situ Cell Death Detection Kit*, Fluorescein (Roche Applied Science, Amadora, Portugal). Briefly, K-562 cells were treated for 72 h with complete medium (blank), the solvent of the compounds (DMSO 0.2% v/v, control), or compound **5** (10 or 20 $\mu$M), as described previously. Cells were then harvested, fixed in 4% paraformaldehyde in PBS, and cytospins were prepared. Cells were permeabilized (0.1% Triton X-100 in 0.1% sodium citrate) and incubated with TUNEL reaction mix, according to the optimized procedure recommended by the manufacturer (enzyme dilution 1:20). Vectashield mounting medium for fluorescence with DAPI (Vector Laboratories, Inc) was used for nuclear counter staining. Cells were observed in a LEICA DM2000 microscope (LEICA), and a semiquantitative evaluation was performed by counting a minimum of 300 cells per slide.

### Protein expression analysis by Western blot

For analysis of protein expression, K-562 cells were treated with complete medium (blank), the solvent of the compound (DMSO 0.2% v/v, control) or with 10 or 20 $\mu$M of compound **5**, as described previously, and processed 72 h after incubation. Cells were lysed in Winman's buffer (1% NP-40, 0.1 M Tris-HCl pH 8.0, 0.15 M NaCl and 5 mM EDTA) with EDTA-free protease inhibitor cocktail (Boehringer, Mannheim). Proteins were quantified using the DC Protein Assay kit (BioRad, Hercules, CA, USA) and separated in 8% or 12% *tris*-glycine sodium dodecyl sulfate (SDS)-polyacrylamide gels (18). Proteins were then transferred to a nitro-cellulose membrane (GE Healthcare, Madrid, Spain). The membranes were incubated with the following primary antibodies for poly (ADP-ribose) polymerase (PARP) (1:4000, Santa Cruz Biotechnology Inc., Heidelberg, Germany), Actin (1:2000, Santa Cruz Biotechnology Inc), Bcl-xL (1:200, Santa Cruz Biotechnology Inc), Bid (1:200, Santa Cruz Biotechnology Inc), and further incubated with the respective secondary

antibodies- horseradish peroxidase (HRP) conjugated (1:2000, Santa Cruz Biotechnology). The signal was detected with the Amersham ECL kit (GE Healthcare), Hyperfilm ECL (GE Healthcare) and Kodak GBX developer and fixer twin pack (Sigma) as previously described (19–21). The intensity of the bands obtained in each film was further analyzed using the software *Quantity One – 1D Analysis* (Bio-Rad).

### *Docking studies*

Structures of several apoptosis pathway proteins were collected from Protein Data Bank, namely *1ysw* (structure of the anti-apoptotic protein Bcl-2 complexed with an acyl-sulfonamide-based ligand), *1ysn* (anti-apoptotic protein Bcl-xL complexed with an acyl-sulfonamide-based ligand), *1g5j* (Bcl-xL in complex with Bad), *1pq1* (Bcl-xL in complex with Bim), *3fdl* (Bcl-xL in complex with BH3 Bim), *2yxj* (Bcl-xL in complex with ABT-737), and *3d7v* (crystal structure of Mcl-1 in complex with an Mcl-1 selective BH3 ligand); *2k7w* and *1f16* (pro-apoptotic protein Bax), *2yv6* (pro-apoptotic protein Bak), *2bid* (pro-apoptotic protein Bid), and *2jk7* (XIAP BIR3 bound to a SMAC mimetic). Virtual screening was carried out on a workstation with Intel Pentium processor, 3.00 GHz, 512 KB cache, 120 GB hard drive and Nvidia Geforce 6600 GT graphic card running Linux Ubuntu 6.06. eHiTS 2009 (22,23) from SimBioSys Inc. was used for active site detection and docking. Hyperchem (24) was used to draw and optimize the structures of the pyranoxanthone **5** and of several known Bcl-2 family antagonists (Table 1). Open Babel (25) was used for manipulating the various chemical formats of ligands. PyMol from DeLano Scientific (26) and Chimera from UCSF (27) were used for visual inspection of results and graphical presentations.

No special preparation of the 3D structures was carried out because eHiTS automatically evaluates all of the possible protonation states for ligands and receptor. eHiTS ran using the crystallographic ligand or the whole protein as clip file. In the first case, the program automatically detected the ligand and selected the part of enzyme within a 7-Å margin around this ligand to be the active site. The known Bcl-2 antagonists and the pyranoxanthone **5** were then docked to the active site using the intermediate mode of docking (accuracy set to 2). The affinity of each molecule to the receptor was determined by a scoring function, eHiTS_Score, which is included in the eHiTS software package.

## Results

### *Synthesis*

The generation of appendance diversity was achieved by different synthetic pathways for 3,4-dihydroxyxanthone (**4**) holding a pyrano ring (**5**), prenyl groups (**6**), a bromohexyl chain (**7**), and a conyferil unit (**8**), as represented in Figure 2. The structures of compounds **4**–**8** were established by spectroscopic methods (IR, $^{1}H$ and $^{13}C$ NMR, HMBC and HSQC) and mass spectrometry.

Compound **4** (Figure 2) was prepared through condensation by Friedel–Crafts acylation (Figure 2 **a**) of an appropriate substituted benzoyl chloride with a phenolic derivative followed by the nucleophilic addition–elimination cyclization step (Figure 2 **b**) of the 2,2′-dioxygenated benzophenone. The demethylation of the corresponding dimethoxylated xanthone (Figure 2 **c**) afforded compound **4** in moderate yield (70%) (27). The synthetic approach used to obtain the pyranoxanthone **5** was by treatment of **4** with prenyl bromide in alkaline medium under reflux (12). At room temperature under similar conditions, the same building block furnished the diprenyl derivative **6** (Figure 2 **e**). Recently, the combination of microwave-assisted synthesis with the use of inorganic solid supports as catalysts, either with solvent or under solvent-free conditions, provided the synthesis of prenylated xanthones with enhanced reaction rates and high yields (28). Coupling of microwave irradiation and montmorillonite K10 clay was successfully applied herein to the synthesis of compound **5**, with a drastic increase in the yield of product as well as the decrease in the reaction time (Figure 2 **f** and experimental conditions). Also the synthesis of linear *O*-prenylxanthones such as compound **6** can be optimized by applying microwave irradiation (28). 3-[(6-Bromohexyl)oxy]-4-hydroxyxanthone (**7**) was obtained as the major product of the drop-wise addition of dibromohexane to **4** (Figure 2 **g**). The synthetic approach for the xanthonolignoid **8** was based on the oxidative coupling of **4** with coniferyl alcohol (**9**) (Figure 2 **h**). The mixture of *trans* and *cis* isomers of (±)-3′-hydroxymethyl-2′-(4′′-hydroxy-3′′-methoxyphenyl)-1′,4′-dioxane[5′,6′-c]xanthone thus obtained was treated with anhydrous $K_2CO_3$ to yield exclusively the *trans* isomer **8** (Figure 2 **i**) (29).

The structures of compounds were established by 2D NMR techniques such as Correlation Spectroscopy (COSY), HSQC, and HMBC, which established the connectivities of the substituents on the xanthone scaffold (**5**–**8**) as well as the orientation on the 1,4-dioxane ring (**8**). Nuclear Overhauser Effect (NOE) experiments were used to determine the stereochemistry of compound **8**.

### *Effects of compounds 4–8 on viable cell number*

The effect of the xanthones **4**–**8** was tested in the K-562 cell line, derived from a blastic phase of human chronic myelogenous leukemia, by verifying the number of viable cells using the trypan blue exclusion assay. These effects were assessed with concentrations ranging from 0 to 20 $\mu$M for 24, 48, or 72 h. Results were compared with those obtained with appropriate controls: DMSO control (solvent of the compounds, 0.2% v/v) and blank treatment (cells incubated with complete medium). All the compounds caused some degree of reduction in the number of viable cells (Figure 3). Results also reveal that compound **5** is the most potent, causing a dose- and time-dependent reduction in viable cell number and presenting an $IC_{50}$ (concentration that inhibits 50% of viable cell number) of 20 $\mu$M upon a 72-h treatment (Figure 4A).

Furthermore, the effect of the pyranoxanthone **5** on viable cell number was investigated in two additional leukemia cell lines: HL-60 and BV-173 (Figure 4B and C, respectively). The results were compared to those previously obtained in the K-562 cell line (Figures 3 and 4A). Compound **5** was capable of reducing the number of viable cells in HL-60 ($IC_{50} \sim 6$–$7$ $\mu$M at both 48 and 72 h, Figure 4B) and BV-173 ($IC_{50} \sim 14$ $\mu$M following 72 h, Figure 4C), presenting $IC_{50}$ values lower than those obtained in the K-562 cell line.

**Table 1:** The structures of non-peptidic antagonists of Bcl-2 and Bcl-xL

| | | |
|---|---|---|
| 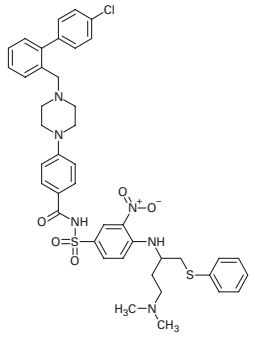 | 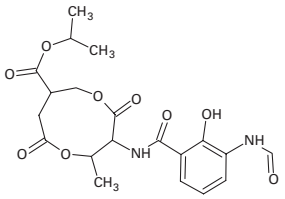 | 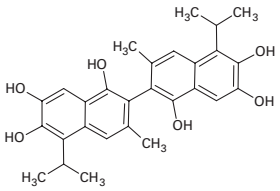 |
| **ABT-737** | **Antimycin A3** | **Apogossypol** |
| 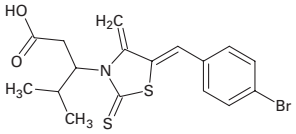 | 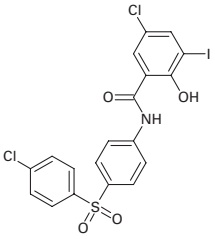 | 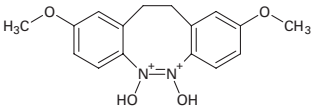 |
| **BH3I-1** | **BH3I-2** | **Dibenzodiazocine derivative** |
| 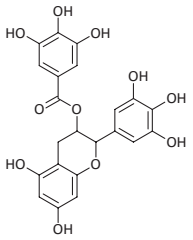 | 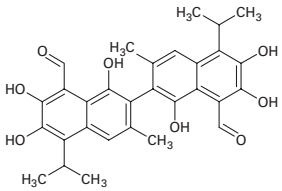 | 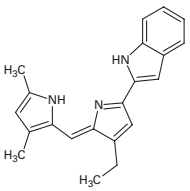 |
| **Epigallocatechin gallate (EGCG)** | **Gossypol** | **GX015-070** |
| 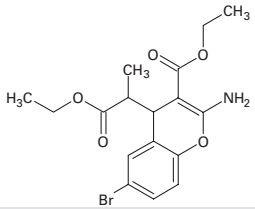 | 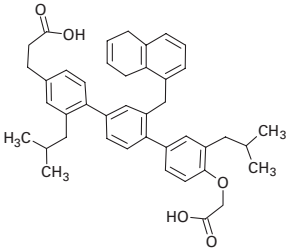 | 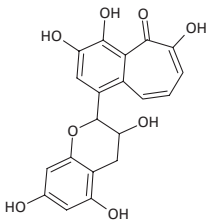 |
| **HA14-1** | **Terphenyl** | **Theaflavanin** |

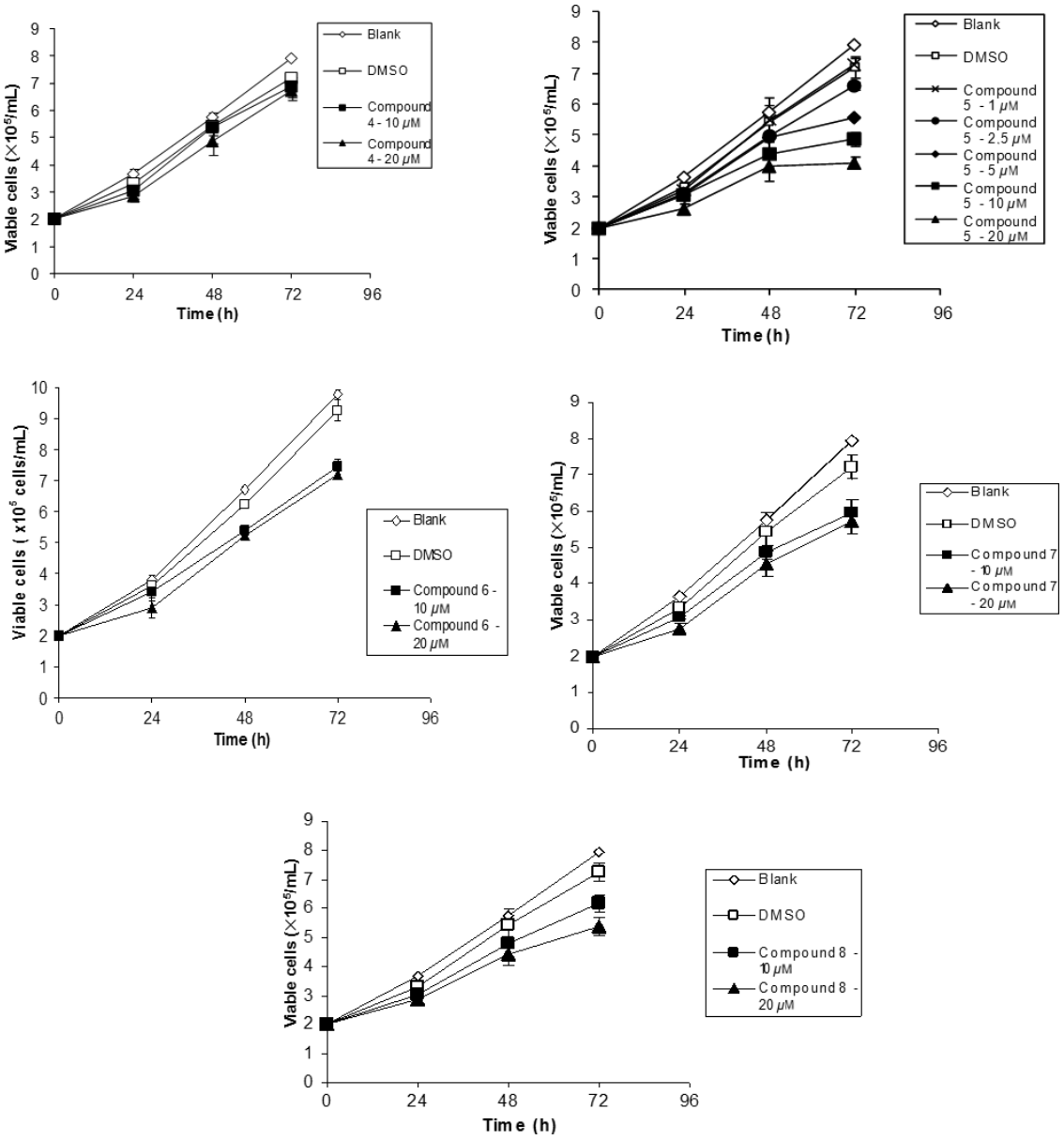


**Figure 3:** Response of K-562 cells to compounds **4**–**8**. K-562 cells were treated with several concentrations of **4**–**8**, with complete medium (blank), or with DMSO control for 24, 48 or 72 h. Viable cell number was determined by the trypan blue exclusion assay. Results are expressed as the mean ± SE of three independent experiments.

Additionally, compound **5** was further tested in an immortalized fibroblast cell line (MRC-5) and no alterations in the viable cell number were observed during 72 h of treatment at 10 or 20 $\mu$M (data not shown), suggesting that this compound preferentially reduces the growth of these leukemia cells.

### *Further characterization of the cellular effects of 3,4-dihydro-12-hydroxy-2,2-dimethyl-2H,6H-pyrano[3,2-b]xanthen-6-one (5)*

To understand the mechanism of action of the pyranoxanthone **5**, cellular proliferation, cell cycle, and apoptosis were studied in the K-562 cell line.

The effect of the pyranoxanthone **5** on cellular proliferation of K-562 cells was determined by using the BrdU incorporation assay. The proliferation levels were calculated as the percentage of cells undergoing proliferation. Results show that cells treated with 10 or 20 $\mu$M of compound **5** for 72 h incorporated less BrdU than the appropriate control cells. The levels of proliferation decreased from 30.8% to 26.2% or 16.9%, after treatment with 10 or 20 $\mu$M of compound **5**, respectively (Figure 5).

Analysis of the effect of the pyranoxanthone **5** on cell cycle was performed by flow cytometry. Compound **5** showed a dose- and time-dependent increase in the percentage of cells in the S-phase of the cell cycle, with a concomitant decrease in cells in

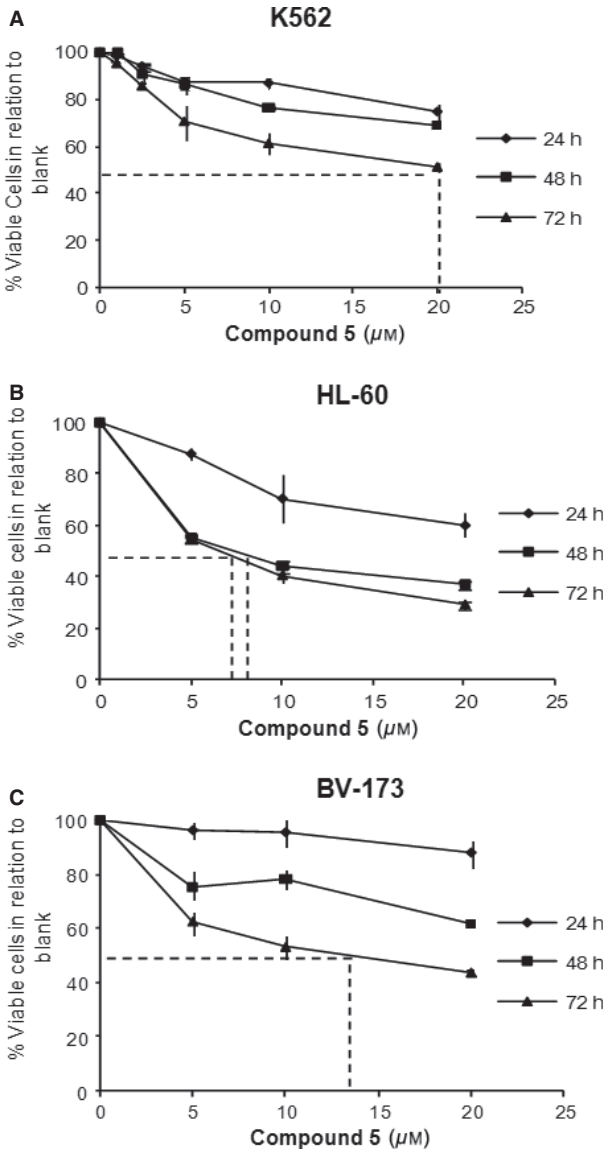


**Figure 4:** Response of three leukemia cell lines to the pyranoxanthone **5**. K-562, HL-60 and BV-173 cells were treated with compound **5** for 24, 48 and 72 h. Viable cell number was analyzed with the trypan blue assay. Plots represent the percentage of viable cells (as a % of the blank cells) against the concentration of compound **5**. Data for the K-562 cell line correspond to that shown in Figure 2. The broken line indicates the $IC_{50}$. (A) Effects of compound **5** on K-562 cell line, (B) on HL-60 cell line, and (C) on BV-173 cell line. Each data point represents the mean ± SE obtained from three independent experiments. Appropriate controls with DMSO were included in the experiments (data not shown).

the G2/M phase (Figure 6). The pyranoxanthone **5** therefore seems to be a strong inducer of S-phase cell cycle arrest, after 72 h of treatment, exhibiting an almost complete loss of cells in G2/M.

Additionally, it was investigated whether compound **5** induced apoptosis in the K-562 cell line, by the TUNEL assay. Results show that increasing concentrations of this xanthone derivative caused increased DNA fragmentation, with the levels of apoptosis rising from 1.3% (DMSO control) to 4.1% or 7.0% after treatment with 10 or 20 $\mu$M of compound **5**, respectively (Figure 7).

The effect of the pyranoxanthone **5** on the expression of some proteins involved in the apoptotic process was determined by Western blot. Results show that incubation with this compound leads to a dose-dependent decrease in PARP with concomitant increase of the cleaved form of this protein (cleaved PARP, Figure 8A). Additionally, a small decrease in the expression levels of anti-apoptotic Bcl-xL (Figure 8B) and an increase in the expression of the pro-apoptotic protein Bid (Figure 8C) were also detected upon compound **5** treatment. Any possible alteration in the levels of expression of Bcl-2, Bak, and XIAP was not conclusive (data not shown).

To further understand the possible mechanism of action of the pyranoxanthone **5** and its involvement in the apoptotic intrinsic pathway, a docking study was performed using the software eHiTS 2009 (22,23). For each protein to be analyzed, we employed crystal structures retrieved from the Protein Data Bank, PDB (30), and Table 2 lists the docking scores (kJ/mol) of the ligands against the Bcl-2 family proteins studied (along with the PDB IDs) Table S1 (in Supporting Information) presents the docking scores (kJ/mol) of the pyranoxanthone **5** against other proteins involved in the apoptotic intrinsic pathway.

The docking scores of known Bcl-2 family antagonists (Tables 1 and 2) were used as positive controls. Fifty unrelated molecules, randomly chosen from the NCI compound database, were used as negative controls (Table S2, Supporting Information). Docking is a method that predicts the preferred orientation of a ligand to a protein, when bound to each other, to form a stable complex. In turn, knowledge of the preferred orientation may be used to predict the binding affinity between them, using scoring functions. In general, the docking score is (or can be related to) the $\Delta G$ for complex formation. A negative score indicates that the complex formation is energetically favorable and the more negative the value, the better would be the binding affinity. The 50 unrelated compounds used as 'decoys' (Table S2, Supporting information) showed higher scores than any of the positive controls and test molecule (>−15 kJ/mol). The pyranoxanthone **5** once docked to Bcl-xL holds scores similar to known Bcl-xL inhibitors (Table 2). Compound **5** docks to the same binding pocket as the known Bcl-xL inhibitor ABT-737 (pdb code *2yxj*) (Figure 9). Additionally, compound **5** establishes interactions within the cavity where BH3-only proteins such as Bim (*3fdl*) and Bad (*1g5j*) bind (Figure 10), suggesting that it may block the formation of a complex between anti-apoptotic Bcl-xL and pro-apoptotic proteins. Scoring results for compound **5** were also in the same order of magnitude as the controls (known Bcl-2 family inhibitors) for other members of the Bcl-2 family (Table 2).

## Discussion

A large group of xanthones has been described as having antitumor properties namely in leukemia models (1). Based on natural

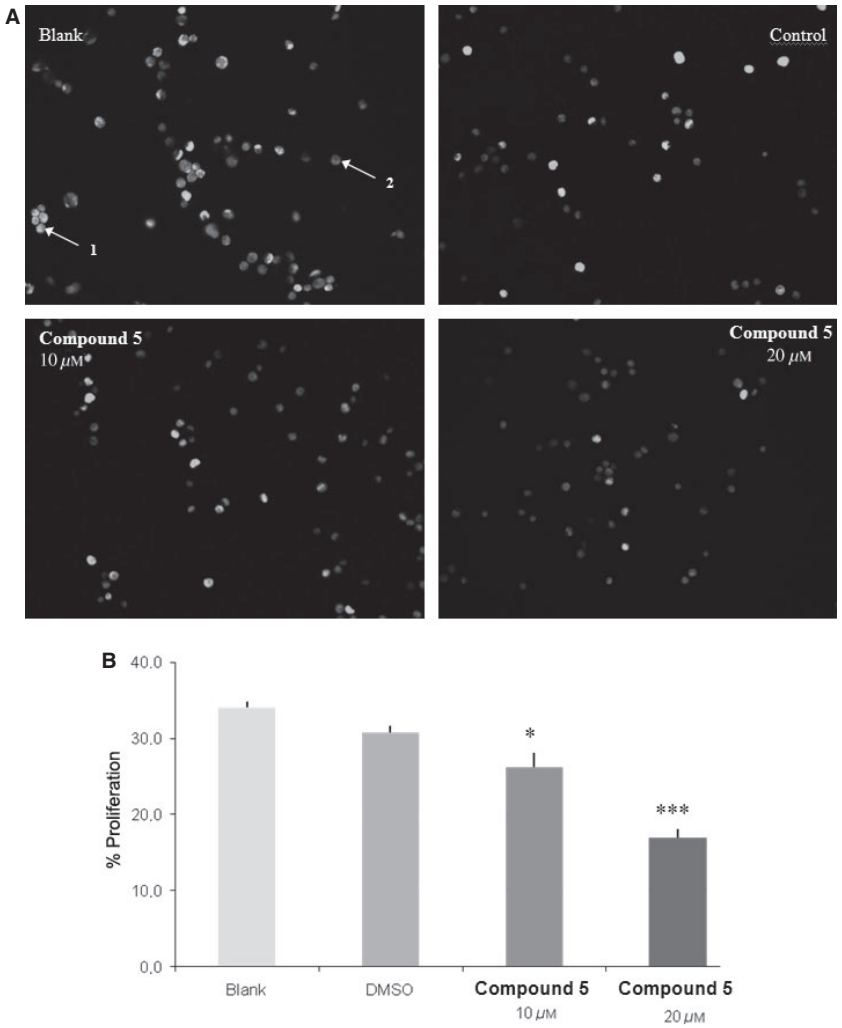


**Figure 5:** Effects of the pyranoxanthone **5** in proliferation of K-562 cells. K-562 cells were treated for 72 h with complete medium (blank), DMSO (control) or with 10 or 20 $\mu$M of compound **5**. The BrdU incorporation assay was used to detect proliferation and cells were analyzed under a fluorescent microscope. (A) Representative photographs of the treated cells. Nuclei are labeled with DAPI. A typical BrdU-positive cell is labeled with the arrow 1 and a typical BrdU-negative cell is labeled with the arrow 2. (B) Semi-quantitative evaluation was carried out by counting a minimum of 300 cells per treatment in each independent experiment. Results are expressed as the mean ± SE of three independent experiments. Statistical significance was tested by paired *t*-test using the DMSO as a negative control. ***Indicates $p < 0.001$; *Indicates $0.01 < p < 0.05$.

prenylated xanthones (12,31), and other analogues with antitumor activity (16,29), structural modifications were produced on the hit compound, 3,4-dihydroxyxanthone (**4**) (15), to prepare four active compounds (**5**–**8**). The present work shows that these derivatives have improved the ability to reduce the viable cell number of K-562 leukemia cells when compared to 3,4-dihydroxyxanthone (**4**). Compound **5**, which includes a pyrano ring at the [3,2-b], was the most potent compound. The synthesis of compound **5** was improved by solid-phase catalysis and microwave-assisted synthesis, to get better yield and shorter reaction time (Figure 2, experimental section).

The results reported here demonstrate that the pyranoxanthone **5** can reduce the number of viable cells of other leukemia cell lines. Compound **5** is particularly active in HL-60 cells, a model of human acute promyelocytic leukemia, when compared to BV-173 and K-562 cells, blastic phase human chronic myelogenous leukemia. The reason for this is most likely related to either: (i) the different uptake of the compound by the cells or; (ii) the mechanism of action of the compound. Several differences can be found among the leukemia cell lines used, such as documented lack of expression of wt p53 tumor suppressor gene in the HL-60 and K-562 cells (32–34), or constitutive activation of the tyrosine kinase (Abl) in both K-562 and BV-173 cells (26), among others. These differences, along with the mechanism of action of the compound, most likely explain the different $IC_{50}$ values found in the three cell lines. Because the HL-60 cell line is a model of acute promyeloid leukemia, the relatively low $IC_{50}$ value obtained for this cell line is particularly interesting regarding future applications for this compound or its new derivatives. Furthermore, the pyranoxanthone **5** is a promising molecule considering that etoposide, currently used in the clinic, has

previously given us an $IC_{50}$ of 9 $\mu$M upon 48-h treatment of the K562 cell line (35).

The pyran-fused xanthones have been previously found to act selectively at specific phases of the cell cycle (8). In general, the angular analogues, which possess a structural similarity with acronycine (**3**), have been shown to induce a partial accumulation of cells in the G2/M phase of the cell cycle. On the other hand, the linear analogues induced a partial accumulation of cells in the G1 phase of the cell cycle (36). Results presented herein clearly show that treatment of K-562 cells with compound **5**, a linear pyran-fused xanthone, caused a concentration- and time-dependent delayed progression of the K-562 cells through the S-phase of the cell cycle, resulting in an S-phase cell cycle arrest with an almost complete disappearance of cells in G2/M.

Further studies of this compound demonstrated that it does not have a detectable effect on the viable cell number of an immortalized fibroblast cell line, within the 72-h incubation period. This finding suggests that leukemia cells are more sensitive to this compound, probably because of the faster growth rate of leukemia cells when compared to the fibroblast cell line. The aforementioned results agree with this hypothesis, because the pyranoxanthone **5** is capable of reducing cellular proliferation by arresting cells in the S-phase of the cell cycle, which will be more evident in cell lines with faster doubling time (growth rate). However, this preference of the compound for leukemia cells should be further confirmed in other 'normal' cellular models.

Several compounds previously showed induction of S-phase arrest, in different types of human cells, including the well-known anticancer agents like cisplatin (37,38), mitomycin C (39,40), hydroxyurea (41,42), and the recent polyphenolic anticancer agent resveratrol (43,44). Several anticancer agents are known to inhibit topoisomerase activity and other key enzymes in DNA duplication (45,46). Furthermore, simple prenylated xanthones have proven to inhibit topoisomerases I and II (47–49) namely psorospermin (**1**) which is, a topoisomerase poison (50,51). Therefore, it would be interesting to further investigate mechanisms of S-phase arrest induced by the pyranoxanthone **5**. Future work may also include research of the levels of cyclin-dependent kinases (CDKs, which govern the progression through the cell cycle) and of the levels of CDK inhibitors (such as p21 or p27), to deeper understand the mechanism of action of this compound.

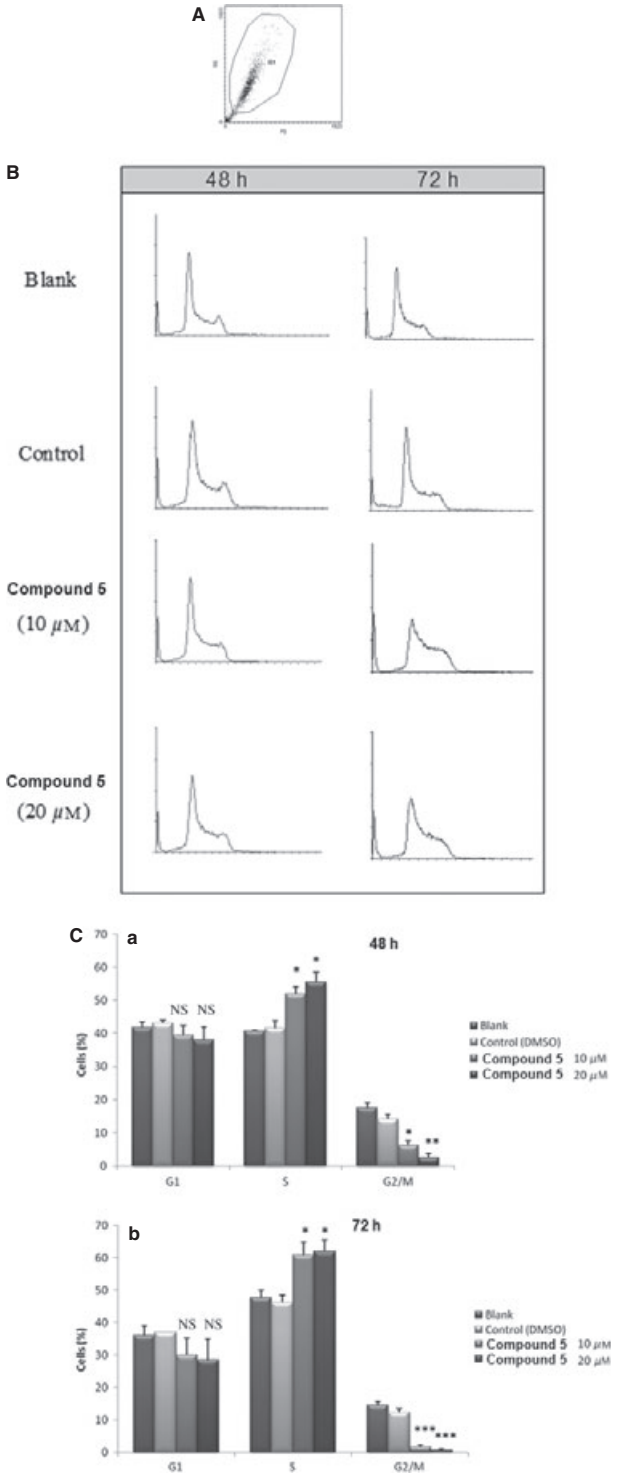


**Figure 6:** Cell cycle analysis of K-562 cells treated with the pyranoxanthone **5**. K-562 cells were cultured with 10 or 20 $\mu$M of compound **5** for 48 or 72 h. Untreated cells were used as control (blank). A DMSO treatment was also included (control). Cell cycle analysis was performed by flow cytometry following propidium iodide staining and a minimum of 50 000 cells were analyzed. (A) Dot plot representing region R1 which was used to trace the histogram. The dot plot is representative of triplicate experiments. (B) Representative histograms of the cell cycle profile of three independent experiments. (C) Graphs representing the differences in the cell cycle distribution of K-562 cells at (**a**) 48 h and (**b**) 72 h following treatment. Results were obtained with the FlowJo 7.2 software. Means ± SE were calculated from triplicates experiments. Statistical significance was tested by paired *t*-test using DMSO as a negative control. ***Indicates $p < 0.001$; **Indicates $0.001 < p < 0.01$; *Indicates $0.01 < p < 0.05$; ns indicates not significant, i.e., $p > 0.05$ ($n = 3$).

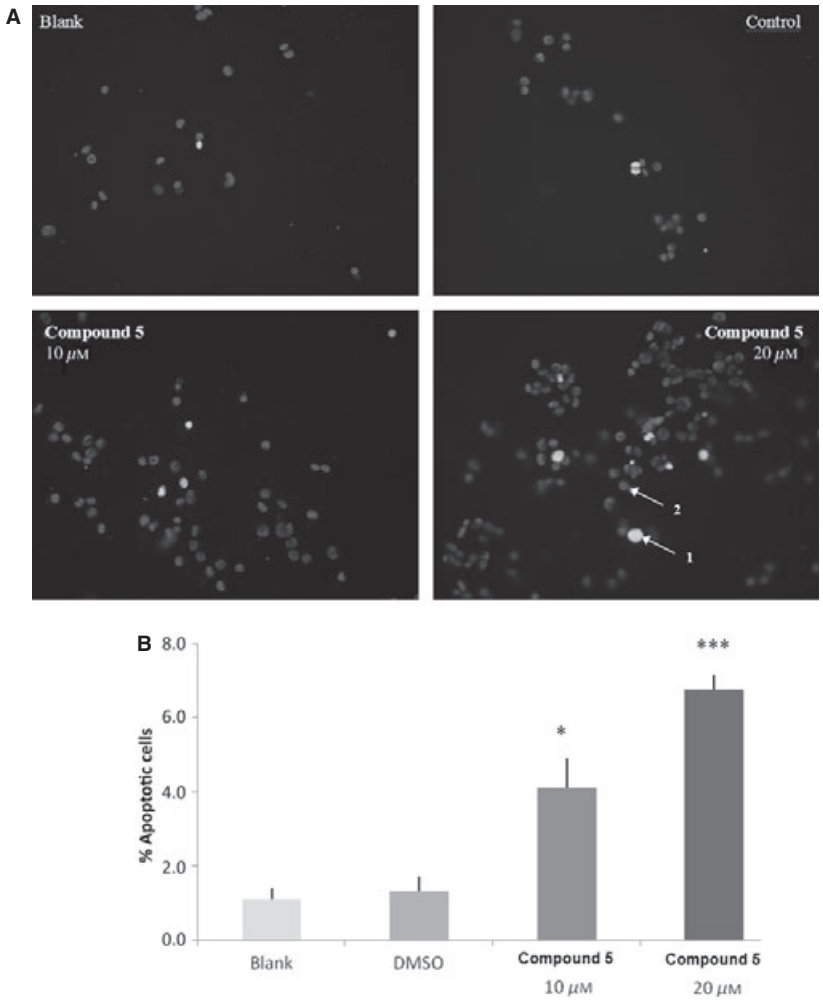


**Figure 7:** Effects of the pyranoxanthone **5** on programmed cell death of K-562 cells. K-562 cells were treated for 72 h with complete medium (blank), DMSO (control) or with 10 or 20 $\mu$M of compound **5**. Programmed cell death was detected by the TUNEL assay. (A) Representative photographs of the treated cells. Nuclei are labeled with DAPI. A typical TUNEL-positive cell is labeled with the arrow 1 and a typical TUNEL-negative cell is labeled with the arrow 2. (B) Semi-quantitative evaluation was carried out by counting a minimum of 300 cells per treatment in each independent experiment. Results are the mean ± SE of three independent experiments. Statistical significance was tested by paired *t*-test using the DMSO as a negative control. ***Indicates $p < 0.001$; *Indicates $0.01 < p < 0.05$.

An increase in programmed cell death was also found following treatment with pyranoxanthone **5**, even though the determined levels of apoptosis were not very high, possibly attributable to the method of detection used (TUNEL). To verify the effective induction of apoptosis, a Western blot analysis showed an evident increase in PARP cleavage following treatment with compound **5** (Figure 8A), indicating that this compound induces cell death by apoptosis in K-562 cells. In accordance with this, it is worth noticing that treatment with compound **5** slightly decreases Bcl-xL (anti-apoptotic) (Figure 8B) and increases Bid (pro-apoptotic) (Figure 8C) levels, which supports the proposal that this compound induces cellular death by apoptosis, namely by inhibition of some Bcl-2 family proteins, directly or indirectly. There was no significant consistent alteration in the levels of expression of Bcl-2, Bak and XIAP (data not shown). Therefore the TUNEL and Western blot assays indicate that the decrease in viable cell number previously observed after treatment with compound **5** was caused, at least in part, by programmed cell death.

A virtual screening on members of the mitochondrial pathway involved in programmed cell death was also performed, to find which ones could be affected by compound **5**. This would provide an indication about compound **5**'s potential as Bcl-2 family antagonist. A docking study of compound **5** against several known Bcl-2 inhibitors and several anti-apoptotic proteins was performed. The pro-survival proteins such as Bcl-2, Bcl-xL and Mcl-1 share four domains of sequence homology known as Bcl-2 homology 1 (BH1), BH2, BH3, and BH4 (52). Other key players that orchestrate apoptosis are the pro-apoptotic BH3-only proteins, such as Bad, Bim and Bid (53,54). The structure of Bcl-xL in complex with the Bad and Bim BH3 domains (Figure 10) sets the foundations for many of the current models for the life and death switch. In fact, in recent

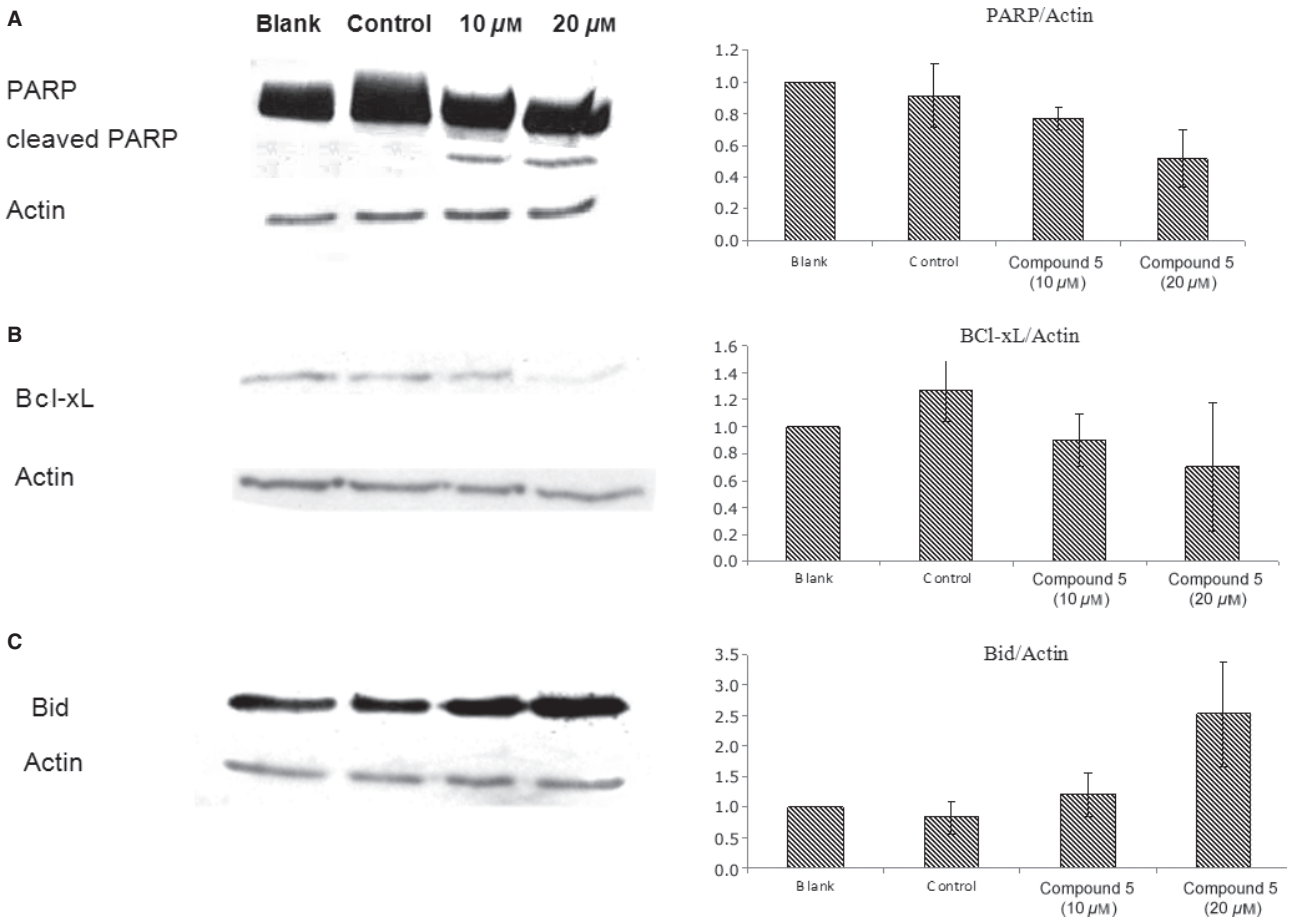


**Figure 8:** The pyranoxanthone **5** alters the expression of some apoptotic proteins. K-562 cells were treated for 72 h with complete medium (Blank), DMSO (control) or with 10 or 20 $\mu$M of compound **5**. Proteins were extracted and analyzed by Western blot. Actin was used as a loading control. The left panel shows representative results and the right panel shows the results of the densitometry analysis, as mean ± SE of at least three independent experiments. (A) Treatment with compound **5** caused cleavage of PARP, (B) a slight reduction in Bcl-xL and (C) increase in Bid.

**Table 2:** Scoring results (kJ/mol) for the pyranoxanthone **5** and several Bcl-2 family antagonists obtained with eHits

| | Bcl-2 (*1ysw*) | Bcl-xL (*1g5j*) | Bcl-xL (*3fdl*) | Bcl-xL (*2yxj*) | Mcl-1 (*3d7v*) |
|---|---|---|---|---|---|
| ABT-737 | −41.69 | −37.26 | −38.10 | −38.35 | −35.02 |
| Antimycin A3 | −23.55 | −22.45 | −23.98 | −24.63 | −22.40 |
| Apogossypol | −28.23 | −34.12 | −33.14 | −32.24 | −38.53 |
| BH3I-1 | −20.67 | −20.54 | −23.59 | −23.77 | −22.02 |
| BH3I-2 | −24.62 | −21.77 | −24.48 | −24.70 | −23.19 |
| Dibenzodiazocine derivative | −19.39 | −19.72 | −20.56 | −20.03 | −19.10 |
| EGCG | −24.65 | −25.85 | −25.29 | −24.70 | −23.40 |
| Gossypol | −28.81 | −30.57 | −37.47 | −30.92 | −37.89 |
| GX015-070 | −22.58 | −21.42 | −23.48 | −22.32 | −22.56 |
| HA14-1 | −20.96 | −19.69 | −22.45 | −24.95 | −18.09 |
| Terphenyl derivative | −30.76 | −37.74 | −37.23 | −33.48 | −33.00 |
| Theaflavanin | −25.84 | −25.07 | −25.58 | −26.18 | −26.64 |
| Pyranoxanthone **5** | −21.58 | −23.52 | −25.13 | −25.17 | −25.98 |

years, several screening studies have been undertaken to find small molecules that could be used as anticancer drugs by binding to Bcl-2 family of proteins (55–60). Results from these studies include the BH3I class of compounds, HA14, ABT-737, gossypol and even the natural product antimycin A. From the obtained results, we hypothesize that the pyranoxanthone **5** may block the binding of anti-apoptotic Bcl-xL to pro-apoptotic Bad or Bim (Figure 10), thus blocking the Bcl-xL/BH3 binding groove (56). Therefore, compound **5** could bind to Bcl-xL protein, triggering apoptosis. However, the indications arising from the results of docking studies must be confirmed experimentally, for example by immunoprecipitation, to determine whether compound **5** is acting directly on Bcl-xL or in any other protein of the apoptotic pathway leading indirectly to decreased levels of Bcl-xL and increased levels of Bid. As shown in Figure 9A–C, compound **5** fits along the ABT-737 binding cavity in spite of being a much smaller molecule than the known inhibitor ABT-737, an organic ligand with high binding affinity for the hydrophobic groove of Bcl-xL (61,62). Therefore, for the design of novel

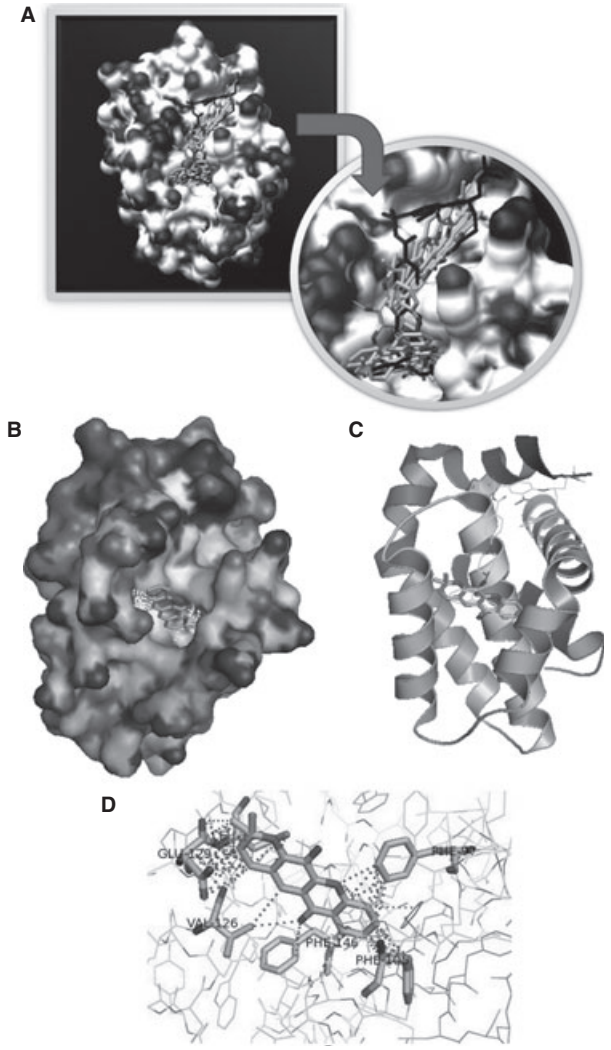


**Figure 9:** Docking poses of the pyranoxanthone **5** on Bcl-xL. (A) Several poses of compound **5** (light gray) docked on the Bcl-xL antagonists docking site; crystallographic inhibitor ABT-737 is represented in black. (B) Surface representation of Bcl-xL and the pyranoxanthone **5** best docking pose; broken white lines represent noncovalent interactions with the receptor. (C) Ribbon representation of Bcl-xL, compound **5** best ranking score (stick) and cristalographic ABT-737 ligand (line). (D) Compound **5** best docking pose on Bcl-xL and important residues involved in the binding.

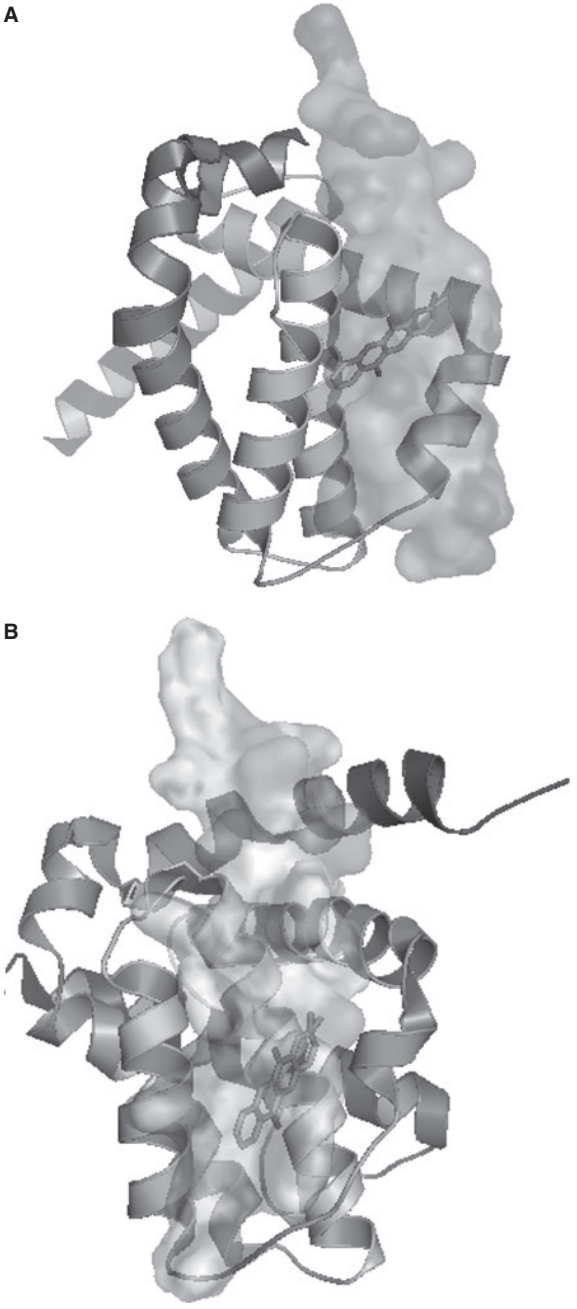


**Figure 10:** Comparison of the pyranoxanthone **5** and pro-apoptotic binding modes on Bcl-xL. Compound **5** best docking pose on Bcl-xL binding site; transparent surface representing the binding of pro-apoptotic protein (A) Bad and (B) Bim.

xanthone derivatives, a good strategy to get even better $IC_{50}$ values could be the molecular extension of the pyranoxanthone **5** to occupy the ABT-737 binding cavity. These docking results represent preliminary data for future optimization studies and the design of novel analogues.

## Conclusion

The results reported here show that the synthetic approaches used were successful in improving the cytotoxicity of 3,4-dihydroxyxanthone (**4**) in leukemia cells. New insights into the antitumor molecular mechanism of action of a new pyranoxanthone were achieved. 3,4-Dihydro-12-hydroxy-2,2-dimethyl-2*H*,6*H*-pyrano[3,2-b]xanthen-6-one (**5**) exhibited antiproliferative and apoptotic effects in leukemia cell lines. The docked geometries of the pyranoxanthone **5**, supported by experimental data, suggest that this molecule may possibly target Bcl-xL.

## Acknowledgments

FCT (I&D, no. 226/2003 and I&D, no. 4040/07), FEDER, POCI, U. Porto and Caixa Geral de Depósitos for financial support. The authors thank Professor Clara Sambade for helpful comments and critical review of the manuscript and Sara Cravo for technical support in microwave equipment.

## References

1. Pinto M.M., Sousa M.E., Nascimento M.S. (2005) Xanthone derivatives: new insights in biological activities. Curr Med Chem;12:2517–2538.
2. Kupchan S.M., Streelman D.R., Sneden A.T. (1980) Psorospermin, a new antileukemic xanthone from Psorospermum febrifugum. J Nat Prod;43:296–301.
3. Rewcastle G.W., Atwell G.J., Li Z.A., Baguley B.C., Denny W.A. (1991) Potential antitumor agents. 61. Structure-activity relationships for in vivo colon 38 activity among disubstituted 9-oxo-9H-xanthene-4-acetic acids. J Med Chem;34:217–222.
4. Jameson M.B., Thompson P.I., Baguley B.C., Evans B.D., Harvey V.J., Porter D.J., McCrystal M.R., Small M., Bellenger K., Gumbrell L., Halbert G.W., Kestell P. (2003) Clinical aspects of a phase I trial of 5,6-dimethylxanthenone-4-acetic acid (DMXAA), a novel antivascular agent. Br J Cancer;88:1844–1850.
5. Hakim E.H., Asnizar, Yurnawilis, Aimi N., Kitajima M., Takayama H. (2002) Artoindonesianin P, a new prenylated flavone with cytotoxic activity from Artocarpus lanceifolius. Fitoterapia;73:668–673.
6. Wu X., Cao S., Goh S., Hsu A., Tan B.K. (2002) Mitochondrial destabilisation and caspase-3 activation are involved in the apoptosis of Jurkat cells induced by gaudichaudione A, a cytotoxic xanthone. Planta Med;68:198–203.
7. Elomri A., Mitaku S., Michel S., Skaltsounis A.L., Tillequin F., Koch M., Pierré A., Guilbaud N., Léonce S., Kraus-Berthier L., Rolland Y., Atassi G. (1996) Synthesis and cytotoxic and antitumor activity of esters in the 1,2-dihydroxy-1,2-dihydroacronycine series. J Med Chem;39:4762–4766.
8. Ghirtis K.P.N., Marakos P., Skaltsounis A.L., Leonce S., Caignard D.H., Atassi G. (2000) Synthesis and Conformational Analysis of Some New Pyrano[2,3-c]xanthen-7-one and Pyrano[3,2-b]xanthen-6-one Derivatives with Cytotoxic Activity. Heterocycles;53:93.
9. Kostakis I.K., Magiatis P., Pouli N., Marakos P., Skaltsounis A.L., Pratsinis H., Léonce S., Pierré A. (2002) Design, synthesis, and antiproliferative activity of some new pyrazole-fused amino derivatives of the pyranoxanthenone, pyranothioxanthenone, and pyranoacridone ring systems: a new class of cytotoxic agents. J Med Chem;45:2599–2609.
10. Kostakis I.K., Pouli N., Marakos P., Mikros E., Skaltsounis A.L., Leonce S., Atassi G., Renard P. (2001) Synthesis, cytotoxic activity, NMR study and stereochemical effects of some new pyrano[3,2-b]thioxanthen-6-ones and pyrano[2,3-c]thioxanthen-7-ones. Bioorg Med Chem;9:2793–2802.
11. Pinto M.M., Sousa E.P. (2003) Natural and synthetic xanthonolignoids: chemistry and biological activities. Curr Med Chem;10:1–12.
12. Castanheiro R.A., Pinto M.M., Silva A.M., Cravo S.M., Gales L., Damas A.M., Nazareth N., Nascimento M.S., Eaton G. (2007) Dihydroxyxanthones prenylated derivatives: synthesis, structure elucidation, and growth inhibitory activity on human tumor cell lines with improvement of selectivity for MCF-7. Bioorg Med Chem;15:6080–6088.
13. Pinto M.M., Castanheiro R. (2008) Natural prenylated xanthones: chemistry and biological activities. In: Brahmachari G., editor. Natural Products: Chemistry, Biochemistry and Pharmacology. New Delhi, India: Narosa Publishing House Pvt. LTD; p. 520–675.
14. Saraiva L., Fresco P., Pinto E., Sousa E., Pinto M., Goncalves J. (2003) Inhibition of protein kinase C by synthetic xanthone derivatives. Bioorg Med Chem;11:1215–1225.
15. Pedro M., Cerqueira F., Sousa M.E., Nascimento M.S., Pinto M. (2002) Xanthones as inhibitors of growth of human cancer cell lines and their effects on the proliferation of human lymphocytes in vitro. Bioorg Med Chem;10:3725–3730.
16. Gottlieb O.R.M., Oliveira G.G., Melo M.T. (1970) Xanthones from Kielmeyera speciosa. Phytochemistry;9:2537–2544.
17. Sousa E.P., Nazareth N., Gales L., Damas A., Nascimento M.S.J., Pinto M. (2009) Bromoalkoxyxanthones as promising antitumor agents: synthesis, crystal structure and effect on human tumor cell lines. Eur J Med Chem;44:1–6.
18. Sambrook J., Fritsch E.F., Maniatis T. (1989) Molecular Cloning: A Laboratory Manual. NY: Cold Spring Harbor.
19. Lima R.T., Martins L.M., Guimaraes J.E., Sambade C., Vasconcelos M.H. (2004) Specific downregulation of bcl-2 and xIAP by RNAi enhances the effects of chemotherapeutic agents in MCF-7 human breast cancer cells. Cancer Gene Ther;11:309–316.
20. Vasconcelos M.H., Beleza S.S., Quirk C., Maia L.F., Sambade C., Guimaraes J.E. (2000) Limited synergistic effect of antisense oligonucleotides against bcr-abl and transferrin receptor mRNA in leukemic cells in culture. Cancer Lett;152:135–143.
21. Lima R.T.G., Vasconcelos M.H. (2007) Overcoming K562Dox resistance to STI571 (Gleevec) by downregulation of P-gp expression using siRNAs. Cancer Ther;5:67–76.
22. Zsoldos Z., Reid D., Simon A., Sadjad B.S., Johnson A.P. (2006) eHiTS: an innovative approach to the docking and scoring function problems. Curr Protein Pept Sci;7:421–435.
23. Zsoldos Z., Reid D., Simon A., Sadjad S.B., Johnson A.P. (2007) eHiTS: a new fast, exhaustive flexible ligand docking system. J Mol Graph Model;26:198–212.
24. Froimowitz M. (1993) HyperChem: a software package for computational chemistry and molecular modeling. BioTechniques;14:1010–1013.
25. O'Boyle N.M., Hutchison G.R. (2008) Pybel: a Python wrapper for the OpenBabel cheminformatics toolkit. Chem Cent J;9:5.
26. Ordog R. (2008) PyDeT, a PyMOL plug-in for visualizing geometric concepts around proteins. Bioinformation;2:346–347.
27. Pettersen E.F., Goddard T.D., Huang C.C., Couch G.S., Greenblatt D.M., Meng E.C., Ferrin TE. (2004) UCSF Chimera-a visualization system for exploratory research and analysis. J Comput Chem;25:1605–1612.
28. Castanheiro R.P., Pinto M.M., Cravo S., Pinto D., Silva A., Kijjoa A. (2009) Improved methodologies for synthesis of prenylated xanthones by microwave irradiation and combination of hetero-

geneous catalysis (K10 clay) with microwave irradiation. Tetrahedron;65:3848–3857.
29. Sousa E.P.S., Pinto M.M., Pedro M.M., Cerqueira F.A.M., Nascimento M.S.J. (2002) Isomeric Kielcorins and Dihydroxyxanthones: Synthesis, Structure Elucidation, and Inhibitory Activities of Growth of Human Cancer Cell Lines and on the Proliferation of Human Lymphocytes In Vitro. Helv Chim Acta;85:2862–2876.
30. Berman H.M., Westbrook J., Feng Z., Gilliland G., Bhat T.N., Weissig H., Shindyalov I.N., Bourne P.E. (2000) The protein data bank. Nucleic Acids Res;28:235–242.
31. Pouli N., Marakos P. (2009) Fused xanthone derivatives as antiproliferative agents. Anticancer Agents Med Chem;9:77–98.
32. Sugimoto K., Toyoshima H., Sakai R., Miyagawa K., Hagiwara K., Ishikawa F., Takaku F., Yazaki Y., Hirai H. (1992) Frequent mutations in the p53 gene in human myeloid leukemia cell lines. Blood;79:2378–2383.
33. Gahmberg C.G., Andersson L.C. (1981) K562-a human leukemia cell line with erythroid features. Semin Hematol;18:72–77.
34. Law J.C.R., Yalowich J.C., Leder G.H., Ferrell R.E. (1993) Mutational inactivation of the p53 gene in the human erythroid leukemic K562 cell line. Leuk Res;17:1045–1050.
35. Lima R.T., Martins L.M., Guimarães J.E., Sambade C., Vasconcelos M.H. (2006) Chemosensitization effects of XIAP downregulation in K562 leukemia cells. J Chemother;18:98–102.
36. Ghirtis K.P., Marakos P., Skaltsounis A.L., Leonce S., Atassi G., Caignard D.H. (2001) Design and synthesis of some new pyranoxanthenones with cytotoxic activity. J Heterocycl Chem;38: 147.
37. Gong J.G., Costanzo A., Yang H.Q., Melino G., Kaelin W.G. Jr, Levrero M., Wang J.Y.J. (1999) The tyrosine kinase c-Abl regulates p73 in apoptotic response to cisplatin-induced DNA damage. Nature;399:806–809.
38. Almeida G.M., Duarte T.L., Farmer P.B., Steward W.P., Jones G.D. (2008) Multiple end-point analysis reveals cisplatin damage tolerance to be a chemoresistance mechanism in a NSCLC model: implications for predictive testing. Int J Cancer;122:1810–1819.
39. Kang S.G., Chung H., Yoo Y.D., Lee J.G., Choi Y.I., Yu Y.S. (2001) Mechanism of growth inhibitory effect of Mitomycin-C on cultured human retinal pigment epithelial cells: apoptosis and cell cycle arrest. Curr Eye Res;22:174–181.
40. Yun J., Zhong Q., Kwak J.Y., Lee W.H. (2005) Hypersensitivity of Brca1-deficient MEF to the DNA interstrand crosslinking agent mitomycin C is associated with defect in homologous recombination repair and aberrant S-phase arrest. Oncogene;24:4009–4016.
41. Hammond E.M., Green S.L., Giaccia A.J. (2003) Comparison of hypoxia-induced replication arrest with hydroxyurea and aphidicolin-induced arrest. Mutat Res;532:205–213.
42. Zhang G.S., Liu D.S., Dai C.W., Li R.J. (2006) Antitumor effects of celecoxib on K562 leukemia cells are mediated by cell-cycle arrest, caspase-3 activation, and downregulation of Cox-2 expression and are synergistic with hydroxyurea or imatinib. Am J Hematol;81:242–255.
43. Estrov Z., Shishodia S., Faderl S., Harris D., Van Q., Kantarjian H.M., Talpaz M., Aggarwal B.B. (2003) Resveratrol blocks interleukin-1beta-induced activation of the nuclear transcription factor NF-kappaB, inhibits proliferation, causes S-phase arrest, and induces apoptosis of acute myeloid leukemia cells. Blood;102:987–995.
44. Tyagi A., Singh R.P., Agarwal C., Siriwardana S., Sclafani R.A., Agarwal R. (2005) Resveratrol causes Cdc2-tyr15 phosphorylation via ATM/ATR-Chk1/2-Cdc25C pathway as a central mechanism for S phase arrest in human ovarian carcinoma Ovcar-3 cells. Carcinogenesis;26:1978–1987.
45. Maga G., Hubscher U. (2008) Repair and translesion DNA polymerases as anticancer drug targets. Anticancer Agents Med Chem;8:431–447.
46. Palchaudhuri R., Hergenrother P.J. (2007) DNA as a target for anticancer compounds: methods to determine the mode of binding and the mechanism of action. Curr Opin Biotechnol;18:497–503.
47. Zhu F.L., Zhou S.N., Vrijmoed L.L.P. (2004) Xanthone Derivatives Isolated from two Mangrove EndophyticFungi #2526 and #1850 from the South China Sea. Nat Prod Res Dev;16:406.
48. Froelich-Ammon S.J., Osheroff N. (1995) Topoisomerase poisons: harnessing the dark side of enzyme mechanism. J Biol Chem;270:21429–21432.
49. Tosa H.I., Tanaka T., Nozaki H., Ikeda S., Tsutsui K., Tsutsui K., Yamada M., Fujimori S. (1997) Inhibitory Activity of Xanthone Derivatives Isolated from some Guttiferaeous Plants Against DNA Topoisomerases I and II. Chem Pharm Bull;45:418–420.
50. Permana P.A., Ho D.K., Cassady J.M., Snapka R.M. (1994) Mechanism of action of the antileukemic xanthone psorospermin: DNA strand breaks, abasic sites, and protein-DNA cross-links. Cancer Res;54:3191–3195.
51. Kwok Y., Hurley L.H. (1998) Topoisomerase II site-directed alkylation of DNA by psorospermin and its effect on topoisomerase II-mediated DNA cleavage. J Biol Chem;273:33020–33026.
52. Adams J.M., Cory S. (1998) The Bcl-2 protein family: arbiters of cell survival. Science;281:1322–1326.
53. Fernandez-Luna J.L. (2008) Regulation of pro-apoptotic BH3-only proteins and its contribution to cancer progression and chemoresistance. Cell Signal;20:1921–1926.
54. Zha J., Harada H., Osipov K., Jockel J., Waksman G., Korsmeyer S.J. (1997) BH3 domain of BAD is required for heterodimerization with BCL-XL and pro-apoptotic activity. J Biol Chem;272:24101–24104.
55. Kang M.H., Reynolds C.P. (2009) Bcl-2 inhibitors: targeting mitochondrial apoptotic pathways in cancer therapy. Clin Cancer Res;15:1126–1132.
56. Lessene G., Czabotar P.E., Colman P.M. (2008) BCL-2 family antagonists for cancer therapy. Nat Rev Drug Discov;7:989–1000.
57. Yip K.W., Reed J.C. (2008) Bcl-2 family proteins and cancer. Oncogene;27:6398–6406.
58. Vogler M., Dinsdale D., Dyer M.J., Cohen G.M. (2009) Bcl-2 inhibitors: small molecules with a big impact on cancer therapy. Cell Death Differ;16:360–367.
59. Azmi A.S., Mohammad R.M. (2009) Non-peptidic small molecule inhibitors against Bcl-2 for cancer therapy. J Cell Physiol;218:13–21.
60. Del Gaizo Moore V., Letai A. (2008) Rational design of therapeutics targeting the BCL-2 family: are some cancer cells primed for

death but waiting for a final push? Adv Exp Med Biol;615:159–175.
61. Chauhan D., Velankar M., Brahmandam M., Hideshima T., Podar K., Richardson P., Schlossman R., Ghobrial I., Raje N., Munshi N., Anderson K.C. (2007) A novel Bcl-2/Bcl-X(L)/Bcl-w inhibitor ABT-737 as therapy in multiple myeloma. Oncogene;26:2374–2380.
62. Del Gaizo Moore V., Schlis K.D., Sallan S.E., Armstrong S.A., Letai A. (2008) BCL-2 dependence and ABT-737 sensitivity in acute lymphoblastic leukemia. Blood;111:2300–2309.

## Supporting Information

Additional Supporting Information may be found in the online version of this article:

**Table S1.** Scoring results (kJ/mol) for the pyranoxanthone **5** and Bax, Bid, Bak and XIAP proteins obtained with eHits.

**Table S2.** Scoring results (kJ/mol) obtained with eHits for 50 'decoy' molecules randomly picked from NCI database.

Please note: Wiley-Blackwell is not responsible for the content or functionality of any supporting materials supplied by the authors. Any queries (other than missing material) should be directed to the corresponding author for the article.